

## Simultaneous Scatterer Shape Estimation and Partial Aperture Far-Field Pattern Denoising

Yaakov Olshansky<sup>1,\*</sup> and Eli Turkel<sup>1</sup>

<sup>1</sup> *Applied Mathematics, Tel-Aviv University, Israel.*

Received 18 November 2009; Accepted (in revised version) 1 December 2010

Available online 24 October 2011

---

**Abstract.** We study the inverse problem of recovering the scatterer shape from the far-field pattern (FFP) in the presence of noise. Furthermore, only a discrete partial aperture is usually known. This problem is ill-posed and is frequently addressed using regularization. Instead, we propose to use a direct approach denoising the FFP using a filtering technique. The effectiveness of the technique is studied on a scatterer with the shape of the ellipse with a tower. The forward scattering problem is solved using the finite element method (FEM). The numerical FFP is additionally corrupted by Gaussian noise. The shape parameters are found based on a least-square error estimator. If  $\tilde{u}_\infty$  is a perturbation of the FFP then we attempt to find  $\Gamma$ , the scatterer shape, which minimizes  $\|u_\infty - \tilde{u}_\infty\|$  using the conjugate gradient method for the denoised FFP.

**AMS subject classifications:** 81U40

**Key words:** Scattering inverse problem, far field pattern.

---

## 1 Introduction

We consider the inverse problem of recovering the scatterer shape from the FFP of the scattered wave. Inverse problems of this type occur in various application such as remote sensing, ultrasound tomography, seismic imaging and radar/sonar detection. They are difficult to solve since they are ill-posed and nonlinear. The ill-posedness is frequently addressed via regularization. Many of the reconstruction methods, such as linear sampling, factorization [4], incorporate some type of regularization.

We propose to directly smooth the (noisy) FFP before the reconstruction. After smoothing, any reconstruction method can be used. For difficult problems, especially with many free parameters, one will frequently require a regularization in addition to the smoothing.

---

\*Corresponding author. *Email addresses:* oyakov@post.tau.ac.il (Y. Olshansky), turkel@post.tau.ac.il (E. Turkel)

However, for the simpler problems presented here no regularization is used. Our technique may be interpreted as an implicit regularization imposed on the FFP rather than on the solution. The efficiency of the proposed technique is demonstrated on the problem of recovering the parameters of the scatterer with the shape of the ellipse with a tower (hard case). This shape may be considered as a simplified imitation of a real submarine. There are three parameters describing the shape in this case: the ellipse semi-axis  $a$  and  $b$  and the height of the tower  $h$  (see Fig. 1).

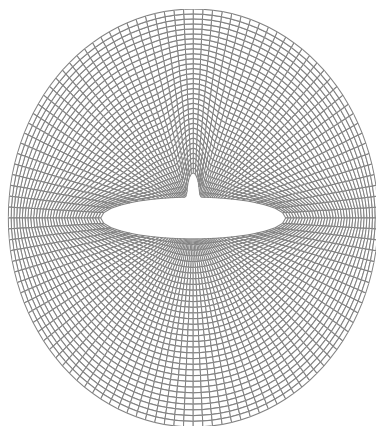


Figure 1: Ellipse with the tower.

## 2 General description of the problem

The problem is formulated as recovering a body shape  $\Gamma$  from the measured FFP. Usually, the body shape  $\Gamma$  is parameterized by a few parameters that should be recovered. The noise source may be either experimental or computational. The problem is complicated by the fact that in practice only a fraction of the data can be obtained. The given FFP is only measured at discrete angles and one can not usually obtain the data in a complete circle/sphere in the far field but only in some portion of the FFP.

We consider the problem for the total wave  $u = u_{inc} + u_s$  in terms of the incoming wave,  $u_{inc} = e^{ikx \cdot d}$ ,  $|d|=1$ , where  $d$  is the direction of the incident plane wave. We solve the reduced wave equation in two dimensions exterior to a given body, so

$$\Delta^2 u + k^2 u = 0, \quad \text{in } \mathbb{R}^2 \setminus \overline{\Omega},$$

where  $\Omega$  is the scattering object. Along the boundary one can impose either a Dirichlet condition corresponding to a sound-soft body or a Neumann condition corresponding to a sound-hard body. In this study we consider an impenetrable sound-hard body and so

$\frac{\partial u}{\partial \nu} = 0$  on  $\Gamma$  the boundary of the obstacle. The far field asymptotic solution is given by

$$u_s(x) = \frac{e^{ikr}}{r^{\frac{1}{2}}} \left[ u_\infty \left( \frac{x}{r} \right) + \mathcal{O} \left( \frac{1}{r} \right) \right], \quad \text{as } r \rightarrow \infty, \quad u_\infty \left( \frac{x}{r} \right)$$

is the FFP. For the forward problem to be well posed we impose the Sommerfeld radiation condition in the farfield. In two dimensions this is given by:

$$r^{\frac{1}{2}} \left( \frac{\partial u_s}{\partial r} - iku_s \right) \rightarrow 0, \quad \text{as } r \rightarrow \infty.$$

The amplitude factor  $u_\infty$  is the far field pattern of the scattered wave. It has been proved in inverse scattering theory [1] that the scattering amplitude, also known as FFP, registers all the information both of physical as well as geometrical character, about the scattering obstacle. The inverse problem is to reconstruct  $\Gamma$  given the FFP. We express this as

$$F(\Gamma) \left( \frac{x}{r} \right) = u_\infty \left( \frac{x}{r} \right).$$

The operator  $F$  assigns to every suitable boundary  $\Gamma$  the corresponding FFP. The inverse problem is not a well-posed problem, i.e. it is well known that adding a small perturbation to the FFP can cause an exponentially large change to the shape of the scatterer [1]. Furthermore, since the scatterer is described by finite number of parameters, in general there will be no solution that exactly matches the given FFP. Hence, we shall only consider a least-squares solution to the problem. If  $\tilde{u}_\infty$  is a perturbation of the exact FFP then we shall attempt to find  $\Gamma$  which minimizes

$$\|u_\infty - \tilde{u}_\infty\|^2.$$

The conjugate gradient method (CG) is used to minimize  $\|u_\infty - \tilde{u}_\infty\|^2$  [2].

### 3 Numerical solution based on the finite element method

We now solve the exterior Helmholtz equation using a finite element code (FEM) with linear elements. If we multiply the Helmholtz equation by a test function  $v$ , integrate over  $D$  and integrate by parts one obtains:

$$\int_D (\nabla u \cdot \nabla v - k^2 uv) dx - \int_{\Gamma_{int}} \frac{\partial u}{\partial \nu} v ds - \int_{\Gamma_{ext}} \frac{\partial u}{\partial \nu} v ds = 0, \quad (3.1)$$

where we denote by  $\Gamma_{int}$  and  $\Gamma_{ext}$  the inner and outer boundaries.

At the inner boundaries we impose a boundary condition on the body  $Bu_s|_{\Gamma_{int}} = -Be^{ikx \cdot d}$  where  $B$  is a boundary operator that characterizes the type of the scatterer. For a sound-soft body  $B$  is a Dirichlet operator and a Neumann derivative operator for a sound-hard body.

At an outer elliptic surface we impose an absorbing boundary conditions using the formula of Kriegsmann et al. [5]

$$\frac{\partial u_s}{\partial v} = iku - \frac{\zeta u_s}{2} - \frac{\zeta^2 u_s}{8(ik - \zeta)} - \frac{1}{2(ik - \zeta)} \frac{\partial^2 u_s}{\partial s^2}, \quad (3.2)$$

where  $\zeta$  is the curvature of the ellipse. The outer ellipse has parameters  $3a, 3b$ , where  $a, b$  are parameters of the ellipse scatterer.

We replace  $D$  by a domain  $D_h$  that consists of a collection of four-node quadrilaterals elements  $Q$  finite elements. We define an  $N \times M$  dimensional subspace  $H^h$  of  $H^1(D_h)$  by constructing an appropriate set of global basis functions  $\varphi_l, l = 1, 2, \dots, N \times M$ . A mesh of  $60 \times 300$  linear elements was used in a polar-like coordinate system around the ellipse and tower. The stiffness, mass and boundary element matrices were calculated by mapping from this generalized polar system to polar coordinates. Refining the grid did not significantly change the results indicating that the waves are well resolved. Our approximation of (3.1) then consists of seeking a function  $u_h$  in  $H^h$ ,

$$u_h = \sum_{j=1}^N u_j \varphi(x_j, y_j), \quad (3.3)$$

such that  $u_j$  unknown coefficients and

$$\int_D (\nabla u_h \cdot \nabla v - k^2 u_h v) dx - \int_{\Gamma_{int}} \frac{\partial u}{\partial v} v ds - \int_{\Gamma_{ext}} \frac{\partial u}{\partial v} v ds = 0, \quad (3.4)$$

where  $v = \varphi_l, l = 1, 2, \dots, N \times M$  is the test function.

Upon substituting (3.3) into (3.4) and simplifying terms, we arrive at the linear algebraic system of equation

$$\sum_{j=1}^N Z_{lj} u_j = F_l, \quad l = 1, 2, \dots, N \times M, \quad (3.5)$$

where  $Z_{ij}$  are

$$Z_{lj} = K_{lj} - k^2 M_{lj} - S_{lj} = \int_D (\nabla \varphi_l \cdot \nabla \varphi_j - k^2 \varphi_l \varphi_j) dx - \int_{\Gamma_{ext}} \frac{\partial u}{\partial v} \varphi_j ds, \quad (3.6)$$

and  $F_l$  are

$$\int_{\Gamma_{int}} \frac{\partial u}{\partial v} \varphi_l ds. \quad (3.7)$$

For Dirichlet conditions, the test function  $v$  is zero on  $\Gamma_{int}$  so the term (3.7) will be zero.

In the matrix form Eq. (3.5) is

$$(M - k^2 K - S) p u = F, \quad (3.8)$$

where  $pu = (u_1, u_2, \dots, u_{N \times M})$  is the obtained scattering solution of (3.5).

The FFP is given by

$$F(a, b, h) = u_\infty(\tilde{x}) = \frac{e^{i\frac{\pi}{4}}}{\sqrt{8\pi k}} \int_{\Gamma_{int}} \left( \frac{\partial u_s(y)}{\partial \nu} + ik\tilde{x} \cdot y u_s(y) \right) e^{-ik\tilde{x} \cdot y} ds, \tag{3.9}$$

where  $\tilde{x} \in S^1 = \{x \in \mathbb{R}^2 \mid |x| = 1\}$  and  $\nu$  is the outward normal to  $\Gamma_{int}$  and  $pu = (u_1, u_2, \dots, u_{N \times M})$  is the obtained scattering solution of (3.5). To compute (3.9) a Gauss quadrature formula was applied.

The FFP is calculated by integrating along  $\Gamma_{int}$  (the scatterer) with the FEM solution  $u_s$  and the calculated  $\frac{\partial u_s}{\partial \nu}$ .

### 4 Nonlinear conjugate gradient method

We consider the problem of minimizing  $f(x)$  for all  $x \in \mathbb{R}^m$ , where  $f(x)$  is a nonlinear function. This is referred to as a non-linear unconstrained optimization problem. The standard approach for solving this problem is to start from an initial approximation  $x_0$  and then to proceed by using an iterative formula of the form:

$$x_{j+1} = x_j + s d_j, \quad j = 0, 1, 2, \dots \tag{4.1}$$

In order to use this formula the values for the scalar  $s$  and the vector  $d_j$  have to be determined. The vector  $d_j$  represents a direction of search and the scalar  $s$  determines how far we should step in this direction. A simple choice for a direction of search is to take  $d_j$  as the negative gradient vector at the point  $x_j$ .

For a sufficiently small step value this can be shown to guarantee a reduction in the function value. This leads to an algorithm of the form

$$x_{j+1} = x_j - s \nabla f(x_j), \quad j = 0, 1, 2, \dots, \tag{4.2}$$

where

$$\nabla f(x) = \left( \frac{\partial f}{\partial x_1}, \frac{\partial f}{\partial x_2}, \dots, \frac{\partial f}{\partial x_m} \right)$$

and  $s$  is a small constant value. This algorithm is called the steepest descent algorithm. The minimum is reached when the gradient is zero.

We can select the step  $s$  which gives the maximum reduction in the function value in the current direction. This procedure is known as a line-search method. This is formally described as minimizing

$$f(x_j - s \nabla f(x_j)) \tag{4.3}$$

in respect to  $s$ . The optimal  $s$  is such that the derivative of  $f(x_j - s \nabla f(x_j))$  with respect to  $s$  is zero. Differentiating  $f(x_j - s \nabla f(x_j))$  with respect to  $s$  leads to:

$$\frac{df(x_j - s \nabla f(x_j))}{ds} = -(\nabla f(x_{j+1}))^T \nabla f(x_j) = 0. \tag{4.4}$$

This shows that with the line search the successive directions of the algorithm are orthogonal.

This is not the fastest way of reaching the optimum value since the changes in successive directions are large; i.e. the overall search path is wobbling. In distinction with the steepest descent method, the conjugate gradient method takes  $d_{j+1}$  a combination of the previous direction  $d_j$  and the negative gradient direction in the new position  $g_{j+1} = \nabla f(x_{j+1})$ :

$$d_{j+1} = -g_{j+1} + \gamma d_j. \quad (4.5)$$

The criterion used for selecting  $\gamma$  is that successive directions of search should be conjugate, i.e.  $(d_{j+1})^T H d_j = 0$  for the Hessian of the function  $f$ , where

$$H = \left[ \frac{\partial^2 f}{\partial x_j \partial x_l} \right]. \quad (4.6)$$

It was shown in Fletcher and Reeves [7] that the requirement of conjugacy leads to a value

$$\gamma = \frac{(g_{j+1})^T g_{j+1}}{(g_j)^T g_j}. \quad (4.7)$$

Thus the conjugate gradient algorithm given by Fletcher and Reeves has the form:

- Step 0: Input value for  $x_0$  and accuracy  $\varepsilon$ . Set  $j=0$  and compute  $d_j = -\nabla f(x_j)$ .
- Step 1: Determine  $s_j$  which is the value of  $s$  that minimizes  $f(x_j + s d_j)$ . Calculate  $x_{j+1}$  where  $x_{j+1} = x_j + s_j d_j$  and compute  $g_{j+1} = \nabla f(x_{j+1})$ . If  $\|g_{j+1}\| < \varepsilon$  then terminate with solution  $x_{j+1}$  else go to step 2.
- Step 2: Calculate new conjugate direction  $d_{j+1}$  where  $d_{j+1} = -g_{j+1} + \gamma d_j$  and  $\gamma$  is given by (4.7).
- Step 3:  $j=j+1$ ; go to step 1.

For a nonlinear function the Polak-Ribiere form of

$$\gamma = \frac{(g_{j+1} - g_j)^T g_{j+1}}{(g_j)^T g_j} \quad (4.8)$$

was shown to be more effective than Eq. (4.7). The conjugate gradient with the Polak-Ribiere form [6] of  $\gamma$  is implemented in function conjgrad.m of the Netlab software [2].

The algorithm terminates when both the change between sequential iteration values and the change in the function values is sufficiently small:

$$\|x_{j+1} - x_j\| < 10^{-6} \quad \text{and} \quad |f(x_{j+1}) - f(x_j)| < 10^{-6}. \quad (4.9)$$

It required 3 iteration for our case. In order to explore a radius of convergence  $R_c = 0.01, 0.02, \dots, 1$ , we consider  $M=4$  initial guesses with

$$a_{init}^l = a + R_c \cos \frac{2\pi l}{M}, \quad b_{init}^l = b + R_c \sin \frac{2\pi l}{M}, \quad h_{init}^l = h + R_c \sin \frac{2\pi l}{M},$$

where  $l = 0, 1, \dots, M-1$  and  $a, b$  are exact ellipse values and  $h$  the height of the tower (Fig. 2).

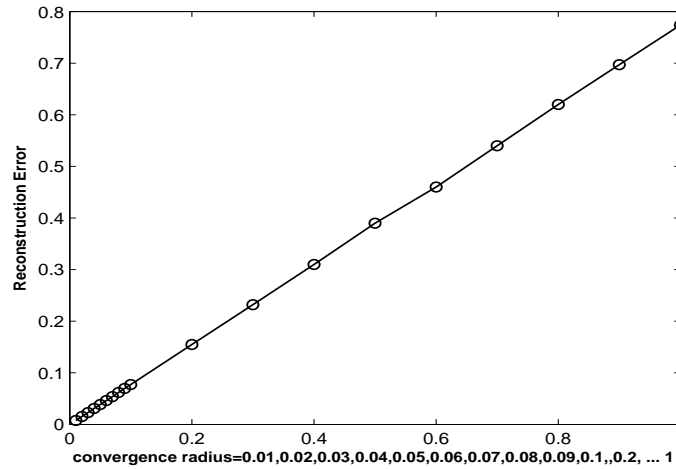


Figure 2: Ellipse with tower of  $a = 5$ ;  $b = 1$ ,  $h = 0.5$ , incident angle  $45^{\circ}$ , wave number  $k = 2$ . Initial guess is  $a = 5 + R_c$ ,  $b = 1 + R_c$ ,  $h = 0.5 + R_c$ . Number of scattering directions 4  $\theta = 61^{\circ}, 68^{\circ}, 69^{\circ}, 70^{\circ}$ .

### 5 Simultaneous smoothing and parameter estimation

Assume that  $f(t)$  is a clean signal and  $F(t)$  is its noisy observation. We further assume:

$$F(t) = f(t) + n(t), \tag{5.1}$$

where  $n(t)$  is independent additive Gaussian noise with a zero mean and variance  $\sigma^2$ . Let the digitized version (discrete representation) of  $F(t)$  sampled at times  $t_i$  be:

$$F_i = f_i + n_i. \tag{5.2}$$

To smooth the noise we replace  $F_i$  by a weighed averaging over its neighbors  $j$ :

$$\hat{F}_i = \sum_{j=i-N}^{i+N} F_j w_{j-i} = \sum_{j=i-N}^{i+N} (f_j + n_j) w_{j-i}, \tag{5.3}$$

where  $2N + 1$  is the length of the filter window and the weights are constrained to be nonnegative and to sum up to one:

$$\sum_{j=-N}^N w_j = 1, \quad w_j \geq 0. \tag{5.4}$$

In Fig. 3 we display an example of  $w_{j-i}$  for  $i = 0$  and so

$$\hat{F}_0 = \sum_j F_j w_j.$$

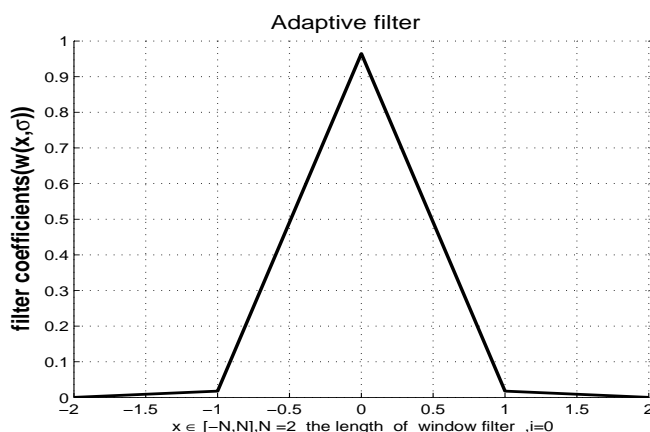


Figure 3: Adaptive filter.

The smoothed value  $\hat{F}_i$  is a normal random variable with mean  $\sum_{j=i-N}^{i+N} f_j w_{j-i}$  and variance  $\hat{\sigma}^2$ :

$$\hat{\sigma}^2 = E\left(\sum_{j=-N}^N n_j w_j\right)^2 = \sigma^2 \sum_{j=-N}^N w_j^2. \quad (5.5)$$

We see from Eqs. (5.4)-(5.5) that  $\hat{\sigma}^2 \leq \sigma^2$  and that the smoothed value  $\hat{F}_i$  has less noise than the original observation  $F_i$ . However, there is a bias in the true estimation of  $f_i$  due to term  $\sum_{j=i-N}^{i+N} f_j w_{j-i}$ . Thus, there is a tradeoff between the noise reduction and the introduced bias. Our goal is to find window coefficients that balance between them.

## 5.1 Optimal weight coefficients

The optimal weight coefficients  $w_{opt}$  should minimize the error between  $\hat{F}_i$  and the real value  $f_i$ :

$$w_{opt} = \underset{w}{\operatorname{argmin}} \hat{E}, \quad (5.6)$$

$$\hat{E} = E\left(\hat{F}_i - f_i\right)^2 = \left(\sum_j w_{j-i} f_j - f_i\right)^2 + \sigma^2 \sum_j w_j^2,$$

where  $w$  satisfies Eq. (5.4). We also constrain the filter to be symmetric  $w_j = w_{-j}$ .

If we know the real signal in advance, an optimal filter is a solution of a quadratic problem (QP)

$$\hat{E} = \left(\sum_j w_{j-i} f_j - f_i\right)^2 + \sigma^2 \sum_j w_j^2, \quad (5.7)$$



with linear constraints

$$w_k \geq 0, \quad \sum_{k=-K}^K w_k = 1, \quad w_k = w_{-k}.$$

However, the signal is not known in advance, but is a parametric analytical function of the ellipse parameters.

The idea is to estimate the ellipse parameters and optimal signal smoothing sequentially until convergence is reached. The ellipse parameters are estimated by minimizing the mean squared error (MSE) between the best "smoothed" observation and ideal parametric FFP. Afterwards the best adaptive filter is found by solving a QP with linear constraints. We use the MINQ software of [3] to find the filter coefficients. Then the obtained filter is used to smooth the signal. In the first iteration, the ellipse parameters are estimated from the noisy data which is equivalent to using the Kronecker filter  $w_j = \delta(j)$ .

## 5.2 Quadratic problem implementation

Let

$$\hat{E} = \left( \sum_{j=-k}^k w_j f_j - f_0 \right)^2 + \sigma^2 \left( \sum_{j=-k}^k w_j^2 \right). \tag{5.8}$$

Then

$$\hat{E} = \left( \sum_{j=-k}^k w_j f_j - f_0 \right)^2 + \sigma^2 \left( 2 \sum_{j=-k}^k w_j^2 + w_0^2 \right), \tag{5.9}$$

$$\hat{E} = \left( \sum_{j=-k}^k w_j (f_{-j} + f_j) - f_0 \right)^2 + \sigma^2 \left( 2 \sum_{j=-k}^k w_j^2 + w_0^2 \right), \tag{5.10}$$

$$\hat{E} = \| (w^t \tilde{f} - f_0) \|^2 + \sigma^2 \left( 2 \sum_{j=-k}^k w_j^2 + w_0^2 \right), \tag{5.11}$$

where  $\tilde{f} = f_{-j} + f_j$ . So that

$$\hat{E} = w^t \tilde{G} w - 2 f_0 \tilde{f}^t w + f_0^t f_0, \tag{5.12}$$

where  $\tilde{G} = \tilde{f}\tilde{f}^t + \sigma^2 D$ ,

$$D = \begin{pmatrix} 2 & 0 & 0 & 0 & \dots & \dots & \dots & \dots & 0 \\ 0 & 2 & 0 & 0 & \dots & \dots & \dots & \dots & 0 \\ 0 & 0 & 2 & 0 & \dots & \dots & \dots & \dots & 0 \\ 0 & 0 & 0 & 2 & \dots & \dots & \dots & \dots & 0 \\ 0 & 0 & 0 & 0 & 2 & \dots & \dots & \dots & 0 \\ \dots & \dots & \dots & \dots & \dots & \dots & \dots & \dots & \dots \\ \dots & \dots & \dots & \dots & \dots & \dots & \dots & \dots & \dots \\ \dots & \dots & \dots & \dots & \dots & \dots & \dots & \dots & \dots \\ 0 & 0 & 0 & \dots & \dots & \dots & \dots & 2 & 0 \\ 0 & 0 & 0 & \dots & \dots & \dots & \dots & 0 & 1 \end{pmatrix}.$$

Translating the constrained condition

$$w_i > 0, \quad \sum_{j=-k}^k w_j = 1 = 2 \sum_{j=-k}^1 w_j + w_0$$

to matrix form yielding

$$\begin{pmatrix} 1 & 0 & \dots & \dots & \dots & \dots & 0 \\ 0 & 1 & 0 & \dots & \dots & \dots & \dots \\ 0 & 0 & 1 & 0 & \dots & \dots & \dots \\ \dots & \dots & \dots & \dots & \dots & \dots & \dots \\ \dots & \dots & \dots & \dots & \dots & \dots & \dots \\ \dots & \dots & \dots & \dots & \dots & \dots & \dots \\ 0 & \dots & \dots & \dots & 0 & 1 & 0 \\ 2 & 2 & 2 & 2 & 2 & 2 & 1 \end{pmatrix} \begin{pmatrix} w_{-k} \\ \dots \\ \dots \\ \dots \\ \dots \\ \dots \\ w_0 \end{pmatrix} \geq \begin{pmatrix} 0 \\ \dots \\ \dots \\ \dots \\ \dots \\ \dots \\ 0 \\ 1 \end{pmatrix}.$$

### 6 Wavelet denoising

This section describes an alternative smoothing technique to that of Section 5. We shall use the wavelet denoising technique [8–11] to smooth the noisy far field before recovering the shape parameters. We represent the FFP using a wavelet expansion

$$f(x) = \sum_{k=-\infty}^{\infty} c_{Jk} \varphi_{Jk} + \sum_{j=J}^{\infty} \sum_{k=-\infty}^{\infty} d_{jk} \psi_{jk}, \tag{6.1}$$

where

$$\begin{cases} c_{jk} = (f, \varphi_{jk}), \\ d_{jk} = (f, \psi_{jk}), \end{cases} \tag{6.2}$$

and  $J$  is the starting index (usually,  $J = 0$ ). It is well known [14] that random noise is mainly located in the  $d$ -coefficients. So by setting the smaller  $d$  coefficients to zero, much

of the noise will be eliminated. This denoising technique was proposed and analyzed by Donoho [8–10] and by Antoniadis [12] and Johnstone [11]. It is often referred to as wavelet shrinkage. A thresholding function  $T_\varepsilon$  is applied to the  $d$ -coefficients:  $d_{nk} \rightarrow T_\varepsilon(d_{nk})$ . The most commonly used thresholding function are hard thresholding

$$T_\varepsilon = \begin{cases} 0, & |x| \leq \varepsilon, \\ x, & |x| > \varepsilon, \end{cases} \quad (6.3)$$

or soft thresholding

$$T_\varepsilon = \begin{cases} x - \varepsilon, & x > \varepsilon, \\ 0, & |x| \leq \varepsilon, \\ -x + \varepsilon, & x < -\varepsilon, \end{cases} \quad (6.4)$$

where  $\varepsilon \in [0, \infty)$  is the threshold parameter. The general de-noising procedure involves three steps:

1. *Decomposition*: Select a wavelet type mother function and the decompose FFP to some level  $N$ .
2. *Thresholding*: Apply thresholding to the  $d$ -coefficients with the threshold parameter selected adaptively per level.
3. *Synthesis*: Reconstruct the signal using the modified  $d$ -coefficients.

The main decisions in using the wavelet technique are the choice of the mother wavelet and the threshold parameter selection technique. We found the symmlet8 [13] mother function to be useful in our application. The threshold parameter  $\varepsilon$  was chosen using soft heuristic SURE thresholding [8–11] and averaged the obtained signals.

## 7 Results

We present results of the reconstruction in the presence of additive Gaussian noise in addition to the computational FFP. We estimate the parameters of the scatterer from the discrete FFP over a partial aperture both with and without smoothing. The results are presented in Figs. 4-6 for an ellipse with an aspect ratio 5:1 and different tower heights  $h = 0.2, 0.3, 0.4, 0.5, 0.6$ . The incident angle in our simulation is taken  $45^\circ$  and the wave number is  $k = 2$ . The reconstruction error  $\mathcal{E}$  between the estimated and the true value is calculated as:

$$\sqrt{\left(\frac{\hat{a} - a}{a}\right)^2 + \left(\frac{\hat{b} - b}{b}\right)^2 + \left(\frac{\hat{h} - h}{h}\right)^2},$$

where  $a$ ,  $b$  and  $h$  are the exact ellipse values and  $\hat{a}$ ,  $\hat{b}$ ,  $\hat{h}$  are the values estimated by the CG method.

Our experiments demonstrate that prior smoothing is useful and improves reconstruction. Pre-smoothing using adaptive filtering led to better results (smaller reconstruction errors) than wavelet de-noising.

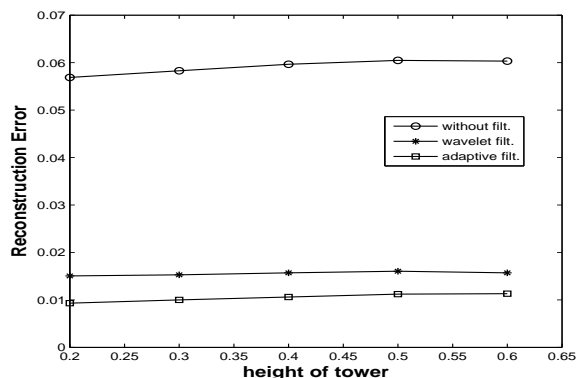


Figure 4: Ellipse with tower of  $a=5$ ;  $b=1$  with 20% Gaussian noise, incident angle  $45^{\circ}$ , wave number  $k=2$ . Initial guess is  $a=5.3$ ,  $b=1.3$ ,  $h = (0.25, 0.35, 0.45, 0.55, 0.65)$ . Number of scattering directions 4  $\theta = 61^{\circ}, 68^{\circ}, 69^{\circ}, 70^{\circ}$ .

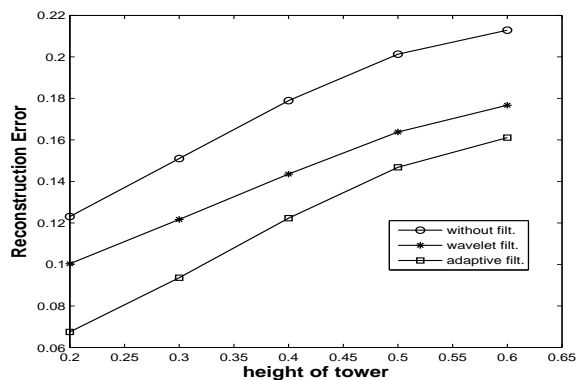


Figure 5: Ellipse with tower of  $a=5$ ;  $b=1$  with 20% Gaussian noise, incident angle  $45^{\circ}$ , wave number  $k=2$ . Initial guess is  $a=5.3$ ,  $b=1.3$ ,  $h = (0.25, 0.35, 0.45, 0.55, 0.65)$ . Number of scattering directions 4  $\theta = 60^{\circ}, 63^{\circ}, 66^{\circ}, 69^{\circ}$ .

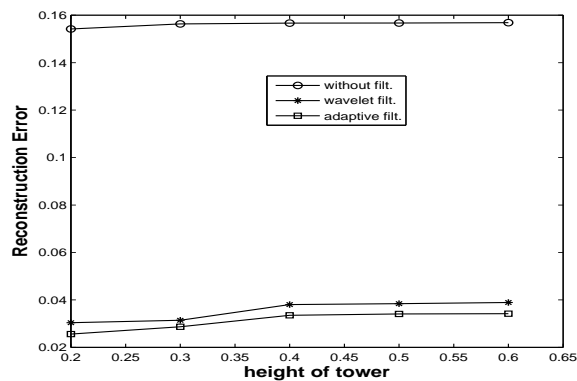


Figure 6: Ellipse with tower of  $a=5$ ;  $b=1$  with 20% Gaussian noise, incident angle  $45^{\circ}$ , wave number  $k=2$ . Initial guess is  $a=5.3$ ,  $b=1.3$ ,  $h = (0.25, 0.35, 0.45, 0.55, 0.65)$ . Number of scattering directions 4  $\theta = 65^{\circ}, 77^{\circ}, 88^{\circ}, 95^{\circ}$ .

We also investigate the dependence of the quality of the reconstruction on the amount of available data. It was found that the minimum number of scattering directions required in the FFP for reconstruction of the scatterer is four. We present three cases with different scattering directions i.e. different aperture angles and different locations of the discrete receivers, but the same minimal number, 4 of directions (i.e. the number of discrete FFP samples). The results are presented in Figs. 4-6.

In the first experiment (Fig. 4), the scattering directions are taken non-uniformly, i.e. the distance between the sequential scattering direction is variable. The scattering direction range is between  $61^{\circ} - 70^{\circ}$ . In the second experiment (Fig. 5), the same interval is covered uniformly by the scattering directions. In the third experiment (Fig. 6), the scattering directions are taken non-uniformly, but their range is extended and lies between  $65^{\circ} - 95^{\circ}$ .

Comparing the two first experiments (Figs. 4, 5), we see that reconstruction from scattering directions with non-uniform sampling leads to better results compared with a uniform sampling. The third experiment (Fig. 6) shows that reconstruction from a larger dynamical range of scattering directions does not improve the results.

We also conducted experiments with the correlated Gaussian noise (Gaussian noise with the non-diagonal covariance matrix). In our experiments the correlated Gaussian noise of increasing level was considered (See Table 1). As the noise level increases the reconstruction error also grows and again the additive filtering was superior to the wavelet de-noising.

Table 1: Reconstruction errors for the ellipse with tower of  $a=5$ ;  $b=1$ ,  $h=0.5$  with correlated Gaussian noise, incident angle  $45^{\circ}$ , wave number  $k=2$ . Initial guess is  $a=5.3$ ,  $b=1.3$ ,  $h=0.55$ . Number of scattering directions 4 ( $\theta=61^{\circ}, 68^{\circ}, 69^{\circ}, 70^{\circ}$ ). The errors  $\mathcal{E}_1$  and  $\mathcal{E}_2$  are estimated with additive and wavelet filtering respectively and  $\mathcal{E}_3$  without filtering.

noise level	5%	10%	15%	20%
$\mathcal{E}_1$	0.0047	0.0093	0.0098	0.0110
$\mathcal{E}_2$	0.0080	0.0101	0.0121	0.0141
$\mathcal{E}_3$	0.0115	0.0289	0.0481	0.0524

## References

- [1] D. Colton and R. Kress, *Inverse Acoustic and Electromagnetic Scattering Theory*, 2nd ed., Springer-Verlag, 1998.
- [2] I. T. Nabney, *Netlab: Algorithms for Pattern Recognition*, Springer Verlag, London, 2004.
- [3] A. Neumaier, *MINQ – General Definite and Bound Constrained Indefinite Quadratic Programming*, WWW-Document, <http://www.mat.univie.ac.at/neum/software/minq/>, 1998.
- [4] D. Colton and R. Kress, Using fundamental solutions in inverse scattering, *Inverse Problems*, 22(3) (2006).

- [5] G. A. Kriegsmann, A. Traflove and K. R. Umashanker, A new formulation of electromagnetic scattering using on surface radiation condition approach, *IEEE Trans. Ant. Prop.* AP35, 42 (1987).
- [6] E. Polak, *Computational Methods in Optimization: A Unified Approach*, Academic Press, New York, 1971.
- [7] R. Fletcher, *Practical Methods of Optimization*, John Wiley, New York, 1987.
- [8] D. L. Donoho, Progress in wavelet analysis and WVD: a ten minute tour, in: *Progress in Wavelet Analysis and Applications*, Y. Meyer, S. Roques Eds., pp. 109-128, 1993, Frontiers Ed.
- [9] D. L. Donoho, De-noising by soft-thresholding, *IEEE Trans. on Inf. Theory*, 41(3) (1995), 613-627.
- [10] D. L. Donoho, I. M. Johnstone, G. Kerkyacharian and D. Picard, Wavelet shrinkage: asymptotia, *J. Roy. Stat. Soc. Series B*, 57(2) (1995).
- [11] D. L. Donoho and I. M. Johnstone, Ideal spatial adaptation by wavelet shrinkage, *Biometrika*, 81(3) (1994), 425-455.
- [12] A. Antoniadis and G. Oppenheim Eds., *Wavelets and Statistics*, Lecture Notes in Statistics 103, Springer Verlag, 1995.
- [13] I. Daubechies, *Ten Lectures on Wavelets*, SIAM, 1992.
- [14] B. Vidakovic, *Statistical Model by Wavelets*, John Willey & Sons, New York, 1999.